Design of Nyquist and Near-Nyquist Pulses with Spectral Constraints

S. Jayasimha and P.K. Singh
Signion Systems Ltd.
20 Rockdale Compound, Somajiguda,
Hyderabad 500082, INDIA
http://www.signion.com

ABSTRACT

Two design procedures, one based on switched pulse shapes, and the other based on alternating projections in the time and frequency domain, are used to obtain interference and jitter-free or reduced interference and jitter (near-Nyquist) pulse-shaping filters. The latter method, that incorporates both frequency- and time- domain constraints into the linear filter design procedure, allows common pulse-shaping filters to be used for both QPSK and 8-PSK used in contemporary satellite modems.

INTRODUCTION

One Intelsat Earth Station Standard [1] using quadrature phase-shift keying (QPSK) requires pulse-shaping (or *filtering*) that, for an R bit per second (bps) non-return-to-zero (NRZ) random bit sequence (with equiprobable 1's and 0's) meets the following:

a) The modulator spectrum lies between certain minimum and maximum spectral *masks* in the range $\pm 0.75R$
b) The filter's group delay should be within $\pm$ 4° from a linear phase shift over a frequency range of $\pm$ $0.25R$ about the nominal center frequency.
c) Outside the bandwidth of $\pm$ $0.75R$ from the nominal center frequency, the transmitted IF spectral density, as measured in a 4kHz bandwidth, shall be at least 40dB below the peak spectral density.

The standard describes a non-mandatory method that achieve these requirements via the cascade of a 6-pole Butterworth filter (BT_s=1.0, B is the 3dB double sided bandwidth of the filter and T_s is the symbol period equal to $2/R$) and a sinc^{-1} compensation filter such the overall BT_s is 1.5. This method suffers from excessive interference and jitter [2].

Direct digital synthesis of the desired pulse shape from impulse ± 1 (*not* NRZ) input is considered in [2], wherein the desired *intersymbol interference-free* (ISI-free) transmission is obtained by forcing the impulse response of the filter to assume zero values for integer multiples of T_s. In the signal processing literature, such impulse responses are called Nyquist or M-th band filters (where, in this case, M represents the number of samples per symbol). A filter whose impulse response, $g(n)$, satisfies:

$$g(n) = \begin{cases} 0, & n = (2N-2)/2 + pM \quad (p = \pm 1, \pm 2, \ldots) \\ \dfrac{1}{M}, & n = (2N-2)/2. \end{cases} \tag{1}$$

is called a M-th band filter. Its frequency response, $G(e^{j\omega})$, satisfies [3]:

$$\sum_{k=0}^{M-1} G(e^{j(\omega + 2\pi k/M)}) = Mg(0) = 1 \tag{2}$$

Several techniques have been devised to design such filters [3-5]. From (2), it is evident that the frequency response of an M-th band filter at π/M is 0.5 (6dB below the nominal passband magnitude). Any spectral mask that does not permit the point (π/M, 0.5) to be a valid frequency response disallows the use of exactly Nyquist filters; in this case, filters that approximately satisfy (1) and (2) and meet the demands of the spectral mask must be designed. In particular, [1] requires that the magnitude response at π/M be at most 4dB below the nominal passband magnitude. We also mention an associated problem, the design of *root-Nyquist* filters. In this case, the receiver transfer function acts in concert with the transmitted pulse to ensure an overall Nyquist characteristic (i.e., the transmit filter is a linear-phase spectral factor of a Nyquist filter). Equiripple root-Nyquist filters that meet the spectral masks required by [1] and [7] can be designed using standard techniques.

SWITCHED ISI- AND JITTER- FREE FILTERS

An alternate method that uses switched filters, based on a decision window of 2 bits, described in [2], which insert sinusoidal transition shapes for each NRZ transition, termed as an ISI- and jitter- free (IJF) response suffers from a similar drawback (see Figures 1 and 2) because its power spectral density (PSD) $S(x)$, where x is a frequency normalized to the symbol rate, derived in Appendix 1, is [2]:

$$S(x) = \left(\frac{\sin 2\pi x}{2\pi x} \cdot \frac{1}{1 - 4x^2} \right)^2 \tag{3}$$

At x=0.5, $S(x)$ is 0.25, or 6dB down from the center frequency. Correcting this by incorporating an inverse sinc function into the switched wave-shapes is possible; with a decision window of 3 symbols, about a 3dB improvement in $S(0.5)$ is obtained (see Appendix 2 and Figure 2) at the expense of the second side-lobe.

This side-lobe must be suppressed by an analog filter or a high-order digital filter. Supporting multiple data rates in the analog filter case increases both cost and space as a selection from a set of installed analog filters must be made. Digital filtering to reduce the second sidelobe increases the complexity of the scheme.

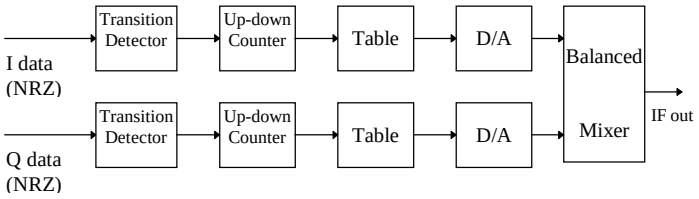

Figure 1. Feher's QPSK-1 Modulator [2]. The tables contain sampled values of $\sin\theta$, $-\pi/2 \le \theta \le \pi/2$.

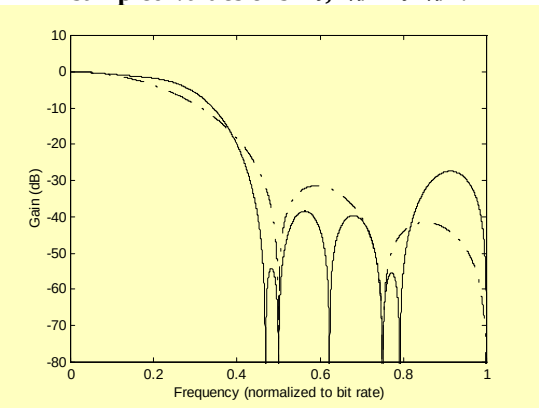

Figure 2. Magnitude response of Feher's QPSK-1 (dashed line) and with IJF/ inverse sinc correction (solid line)

Coefficients for 2- and 3-samples per symbol baseband waveshapes (with inverse sinc correction and corresponding to the middle bit) are shown in Table 1.

Bit Sequence	2-sample waveform	3-sample waveform
000	-1.0000, -1.0000	-c, -c, -c
001	-1.0000, -0.7949	-c, -b, -a
010	0.7949, 0.7949	a, c, a
011	0.7949,1.0000	a=0.50037, b=1.06881, c=1.00000
100	-0.7949,-1.0000	-a, -b, -c
101	-0.7949, -0.7949	-a, -c, -a
110	1.0000, 0.7949	c, b, a
111	1.0000, 1.0000	c, c, c

Table 1. Switched IJF waveforms with inverse sinc correction

Extension of this method to the design of waveshapes for 8-PSK used in [7] requires a 9-bit window on the input bit stream. This 9-bit window is further decomposed into two (redundant) 6-bit windows, one each for the I and Q channels. For each 6 bit pattern, a length 64 table (similar to Table 2) is derived. The table size becomes large for *M*-PSK, M>3; this motivates the use linear interpolation filters (with upsampling factors inversely proportional to bit rate) designed using alternating projections onto time- and frequency- domain convex constraint sets, that output data to a DAC at a constant rate. This may be followed by a single (overall) analog filter. One advantage of this method, discussed in the next section, is that the same filter may be used for both the QPSK of [1] and the 8-PSK of [7].

ITERATIVE DESIGN USING POCS

The iterative method begins by the initial prototype, $h'_0(n)$, which is the inverse Fourier transform of $H_{id}(\omega)$ (a transfer function that meets the spectral mask requirements) i.e., $h_{id}(n)=\mathcal{F}^{-1}[H_{id}(\omega)]$ truncated to support I (in the present case, I is assumed to consist of N contiguous samples):

$$h'_0(n) = \begin{cases} h_{id}(n), & \text{if } n \in I \\ 0, & \text{otherwise.} \end{cases} \tag{4}$$

The frequency response, $H'(e^{j\omega})$, of the zero-phase filter is required to be within prescribed upper and lower bounds in its passband and stopband as follows:

$$H'_{id}(e^{j\omega}) - E_d(\omega) \le H'(e^{j\omega}) \le H'_{id}(e^{j\omega}) + E_d(\omega) \qquad \omega \in F_r \tag{5}$$

where $H'_{id}(e^{j\omega})$ is the ideal filter response, $E_d(\omega)$ is a positive function of ω, which takes values in F_r. Each iteration consists of applying successive temporal and frequency domain constraints to the current iterate. The k-th iteration has the following steps:

- Compute the zero-phase frequency response of the k-th iterate $h_k(n)$ on a suitably dense grid of frequencies using the Fast Fourier Transform (FFT) algorithm
- Impose the frequency domain constraints of (4) on this dense grid of frequencies
- Compute the impulse response associated with this frequency response using an inverse FFT
- Truncate the impulse response to the desired support (3) to obtain $g_k(n)$
- Determine the deviation, $e_k(n)$ of this impulse response from a weaker form of the Mth-band condition of (1)

$$e_k(n) = \begin{cases} g_k(n), & n = \dfrac{N-1 \pm pM}{2} + 1,\ p = 3,5,7,\ldots \\ 0, & \text{else} \end{cases} \tag{6}$$

This condition avoids interference between symbols spaced apart by more than one symbol interval.

- Interpolate this error sequence, $e_k(n)$, by convolving it with $g_k(n)$ and reducing the result's support to N central samples to obtain $f_k(n)$
- Subtract $\alpha \cdot f_k(n)$ from $g_k(n)$ to obtain $h_{k+1}(n)$, where $0<\alpha<1$ is chosen suitably

An iteration termination criterion is when a suitable metric (e.g., L^{∞} norm) between the kth and the $(k+1)$th iterate is less than a threshold. If the frequency domain constraints are too stringent or α is too large, the iteration may not converge; a limit on the number of iterations is recommended. In this event, assuming that the frequency domain constraints are realizable, the support N is increased or α is reduced (or both).

RESULTS

Eye-patterns [2], frequently used to evaluate signal and channel imperfections, are obtained on an oscilloscope if the transmitted (or channel impaired) signal is fed to the vertical input of an oscilloscope while the symbol clock is fed to its external trigger. The *eye-opening* and the *zero-crossings* of the eye pattern are important in determining extra power or the data-transition jitter associated with an imperfect (non-Mth band) data shaping filter. For example, if the eye-opening is reduced by 85%, an equal decision margin requires a 1.4dB signal level increase. Though transition jitter by itself does not necessarily lead to performance degradation, data-transition jitter combined with clock jitter and/ or a static clock offset may lead to significant degradation [6].

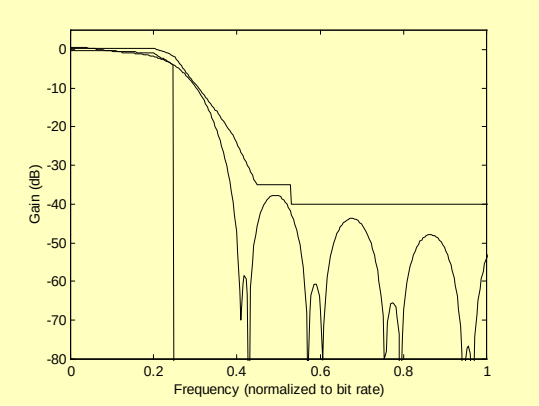

Figure 3. Designed magnitude response shown along with upper and lower spectrum constraints (for QPSK of [1])

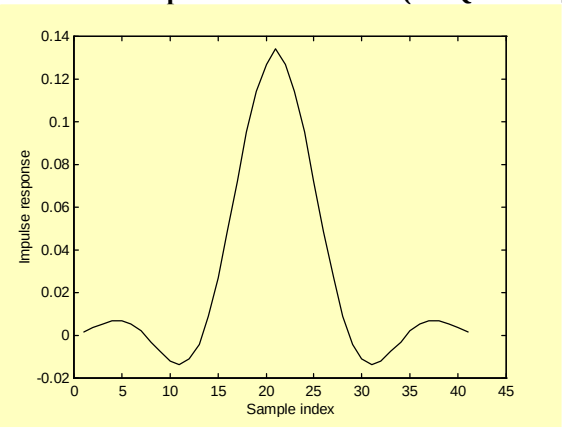

Figure 4. Impulse response (with 5 symbol-duration's support) of designed filter

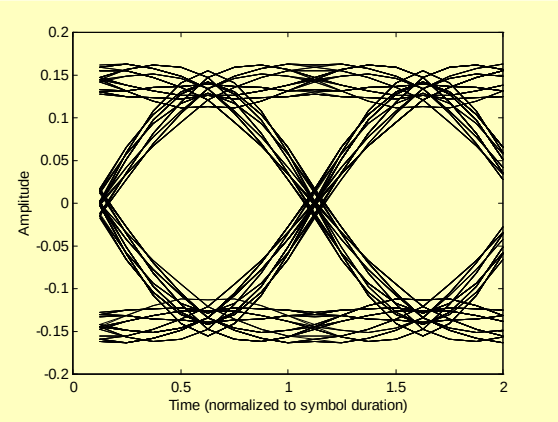

Figure 5. QPSK eye diagram associated with designed filter

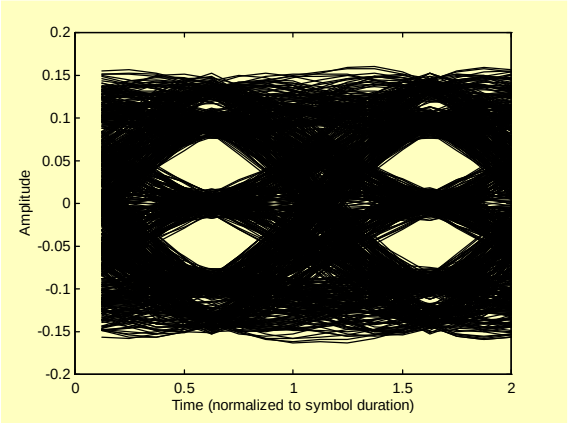

Figure 6. 8-PSK eye diagram associated with designed filter

Coefficient	Value
h(0)=h(40)	1.3402638e-003
h(1)=h(39)	3.8244552e-003
h(2)=h(38)	5.5046170e-003
h(3)=h(37)	6.6868215e-003
h(4)=h(36)	6.5848940e-003
h(5)=h(35)	5.2457689e-003
h(6)=h(34)	1.8887894e-003
h(7)=h(33)	-3.2882370e-003
h(8)=h(32)	-7.1354006e-003
h(9)=h(31)	-1.2081291e-002
h(10)=h(30)	-1.3461233e-002
h(11)=h(29)	-1.1232700e-002
h(12)=h(28)	-3.9701417e-003
h(13)=h(27)	8.6964544e-003
h(14)=h(26)	2.6842589e-002
h(15)=h(25)	4.8345543e-002
h(16)=h(24)	7.2146512e-002
h(17)=h(23)	9.5255840e-002
h(18)=h(22)	1.1428773e-001
h(19)=h(21)	1.2692899e-001
h(20)	1.3418602e-001

Table 2. Impulse response coefficients for M=8, N=41

For the constraints specified in [1], POCS iteration produced a filter with magnitude response (shown along with the frequency domain constraints) as in Figure 3. Its impulse response is shown in Figure 4, while the eye diagrams for QPSK and 8-PSK (used in [7]) is shown in Figures 5 and 6. The eye opening for QPSK is reduced by only about 5% (requiring a signal level increase by only about 0.4dB with the same decision margins as compared to a Nyquist filter. Timing jitter is less than 5%. Table 2 provides numerical values for the impulse response coefficients.

Transmit root-Nyquist filters may be designed using standard techniques without much difficulty as (π/M, $1/\sqrt{2}$) lies within the spectral mask. We have illustrated an equiripple filter that may be designed using the techniques provided in [9] or [10]. The design of receive root-Nyquist filters, using 1 sample per symbol and including a tunable fractional delay component for symbol timing synchronization, are outside the scope of this paper.

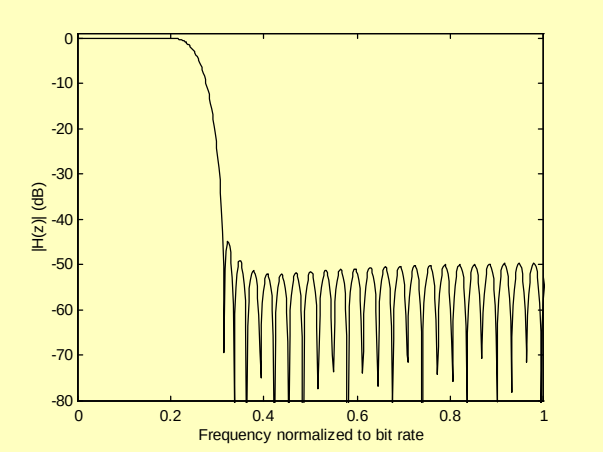

Figure 7. Near-equiripple root-Nyquist magnitude response (a 127-tap FIR filter meets aspectral mask required by [1])

APPENDIX 1

For m=2 symbols decision window, the NRZ signals, $x_I(t)$ and $x_Q(t)$, are encoded into IJF baseband signals $y_I(t)$ and $y_Q(t)$ using:

$$y(t) = \sum_{n=-\infty}^{\infty} y_n(t) \tag{A1.1}$$

where

$$y_n(t) = \begin{cases} s_e(t-nT_s), \text{ if } x_n = x_{n-1} = +1 \\ -s_e(t-nT_s), \text{ if } x_n = x_{n-1} = -1 \\ s_o(t-nT_s), \text{ if } x_n = +1,\ x_{n-1} = -1 \\ -s_o(t-nT_s), \text{ if } x_n = -1,\ x_{n-1} = +1 \end{cases} \tag{A1.2}$$

where $s_e(t\text{-}nT_s)$ and $s_o(t\text{-}nT_s)$ are even and odd single interval pulses satisfying the IJF conditions. The PSD of the encoded signal $y(t)$ is (this PSD has only continuous components; see [8]):

$$Y(f) = \frac{1}{T_s}\sum_{j=0}^{2^m-1}\pi_j \cdot \left|S_j(f)\right|^2 + \frac{2}{T_s}\mathrm{Re}\left[\sum_{j=0}^{2^m-1}\sum_{k=0}^{2^m-1}\pi_j S_j^*(f)\cdot S_k(f)\cdot Q_{jk}(f)\right] \tag{A1.3}$$

where π_j is the stationary probability of state j and Q_{jk} , the generating functions of transition probabilities, p_{jk}, from state j to k, are

$$Q_{jk}(f) = \sum_{n=1}^{\infty} p_{jk}^{(n)} e^{-j2\pi nfT_s} \tag{A1.4}$$

Here,

$$Q_{02} = \frac{1}{4}e^{-4\pi fT_s} + \frac{1}{4}e^{-6\pi fT_s} = \frac{1}{4}\cdot\frac{e^{-j4\pi fT_s}}{1-e^{-j2\pi fT_s}} \tag{A1.5}$$

$$Q_{01} = \frac{1}{2}e^{-j2\pi fT_s} + \frac{1}{4}e^{-4\pi fT_s} + \frac{1}{4}e^{-6\pi fT_s} = \frac{1}{2}\cdot e^{-j2\pi fT_s} + Q_{02} \tag{A1.6}$$

$Q_{03}= Q_{10}= Q_{23}= Q_{30}= Q_{31}= Q_{02}= Q_{11}= Q_{22}$ and $Q_{12}= Q_{13}= Q_{20}= Q_{21}= Q_{32}= Q_{01}= Q_{00}= Q_{33}$. (A1.7)

Substituting (A1.5)-(A1.7) in (A1.3),

$$Y(f) = \frac{1}{2T_s}\left[|S_e|^2+|S_o|^2\right] + \frac{2}{T_s}\mathrm{Re}\left[S_e^* S_o (Q_{01}-Q_{02})\right] - \frac{1}{T_s}\mathrm{Re}\left[Q_{02}|S_e|^2+Q_{01}|S_o|^2\right] + \frac{1}{T_s}\mathrm{Re}\left[Q_{01}|S_e|^2+Q_{02}|S_o|^2\right] \tag{A1.8}$$

After simplification,

$$Y(f) = \frac{1}{T_s}\left[S_e(f)\cos\pi fT_s - jS_o(f)\sin\pi fT_s\right]^2 \tag{A1.9}$$

where

$$S_e = \int_{\frac{-T_s}{2}}^{\frac{T_s}{2}} e^{-j2\pi ft}dt = \frac{T_s\sin\pi x}{\pi x} \tag{A1.10}$$

and for a sinusoidal transition shape

$$S_o = \int_{\frac{-T_s}{2}}^{\frac{T_s}{2}} \sin(\frac{\pi t}{T_s})e^{-j2\pi ft}dt = \frac{-j\cos\pi x\cdot 4\pi xT_s}{\pi^2-(2\pi x)^2} \tag{A1.11}$$

where x=fT_s**.** Obtain (3) by using (A1.10) and (A1.11) in (A1.9).

APPENDIX 2

For m=3 symbols decision window, which allows IJF inverse sinc filters to be incorporated into pulse shapes, the NRZ signals, $x_I(t)$ and $x_Q(t)$, are encoded into IJF baseband signals $y_I(t)$ and $y_Q(t)$ using:

$$y(t) = \sum_{n=-\infty}^{\infty} y_n(t) \tag{A2.1}$$

If subscripts e and o denote even and odd functions respectively and $\tilde{x}$ denotes the time-reversal of x,

$$y_n(t)=\begin{cases} s_0(t-nT_s)=s_{e0}(t-nT_s),\ \text{if } x_n=x_{n-1}=x_{n+1}=+1 \\ -s_0(t-nT_s)=-s_{e0}(t-nT_s),\ \text{if } x_n=x_{n-1}=x_{n+1}=-1 \\ s_2(t-nT_s)=s_{e2}(t-nT_s),\ \text{if } x_n=1,\ x_{n-1}=x_{n+1}=-1 \\ -s_2(t-nT_s)=-s_{e2}(t-nT_s),\ \text{if } x_n=-1,\ x_{n-1}=x_{n+1}=1 \\ s_{e1}(t-nT_s)+s_{o1}(t-nT_s),\ \text{if } x_n=x_{n-1}=+1,\ x_{n+1}=-1 \\ -s_{e1}(t-nT_s)-s_{o1}(t-nT_s),\ \text{if } x_n=x_{n-1}=-1,\ x_{n+1}=+1 \\ \tilde{s}_{e1}(t-nT_s)+\tilde{s}_{o1}(t-nT_s),\ \text{if } x_n=x_{n+1}=+1,\ x_{n-1}=-1 \\ -\tilde{s}_{e1}(t-nT_s)-\tilde{s}_{o1}(t-nT_s),\ \text{if } x_n=x_{n+1}=-1,\ x_{n-1}=+1 \end{cases} \quad \text{(A2.2)}$$

The Fourier transforms of the first 4 possibilities are real, while the latter 4 are complex, with the latter two of these being the complex conjugates of the former two. Considering a shift-register of three bits, the generating functions for the 3-bit shift-register symbols are:

$$Q=\begin{bmatrix} Q_{00} & Q_{00} & Q_{02} & Q_{02} & Q_{04} & Q_{04} & Q_{04} & Q_{04} \\ Q_{04} & Q_{04} & Q_{12} & Q_{12} & Q_{02} & Q_{02} & Q_{02} & Q_{02} \\ Q_{02} & Q_{02} & Q_{02} & Q_{02} & Q_{12} & Q_{12} & Q_{04} & Q_{04} \\ Q_{04} & Q_{04} & Q_{04} & Q_{04} & Q_{02} & Q_{02} & Q_{00} & Q_{00} \\ Q_{00} & Q_{00} & Q_{02} & Q_{02} & Q_{04} & Q_{04} & Q_{04} & Q_{04} \\ Q_{04} & Q_{04} & Q_{12} & Q_{12} & Q_{02} & Q_{02} & Q_{02} & Q_{02} \\ Q_{02} & Q_{02} & Q_{02} & Q_{02} & Q_{12} & Q_{12} & Q_{04} & Q_{04} \\ Q_{04} & Q_{04} & Q_{04} & Q_{04} & Q_{02} & Q_{02} & Q_{00} & Q_{00} \end{bmatrix} \quad \text{(A2.3)}$$

Substituting in (A1.3)

$$\begin{aligned} Y(x)=\frac{1}{8T_s}\Big\{ & 2{S_0}^2(1+\cos 2\pi x+0.5\cos 4\pi x)+4|S_1|^2(1-0.5\cos 4\pi x)+ \\ & 2{S_2}^2(1+0.5\cos 4\pi x-\cos 2\pi x)-2S_0S_2\cos 4\pi x+ \\ & 2\,\mathrm{Re}\left[S_1(2S_0+S_1)(e^{-j2\pi x}+0.5e^{-j4\pi x})\right]- \\ & 2\,\mathrm{Re}\left[(S_1S_2+S_0S_1^*)e^{-j4\pi x}\right]+ \\ & 2\,\mathrm{Re}\left[S_1^*(2S_2+S_1^*)\cdot(0.5e^{-j4\pi x}-e^{-j2\pi x})\right]\Big\} \end{aligned} \quad \text{(A2.4)}$$

Set $S_1=S_{1e}+jS_{1o}$:

$$\begin{aligned} Y(x)=\frac{1}{8T_s}\Big[& 2{S_0}^2(1+\cos 2\pi x+0.5\cos 4\pi x)+4|S_1|^2(1-0.5\cos 4\pi x)+ \\ & 2{S_2}^2(1+0.5\cos 4\pi x-\cos 2\pi x)-2S_0S_2\cos 4\pi x+ \\ & 2\left\{S_{1e}(2S_0+S_{1e})-S_{1o}^2\right\}(\cos 2\pi x+0.5\cos 4\pi x)+ \\ & 4S_{1o}(S_0+S_{1e})(\sin 2\pi x+0.5\sin 4\pi x)\ - \\ & 2S_{1e}(S_2+S_0)\cos 4\pi x-2S_{1o}(S_2-S_0)\sin 4\pi x\ + \\ & 2(2S_{1e}S_2+S_{1e}^2-S_{1o}^2)(0.5\cos 4\pi x-\cos 2\pi x)+ \\ & 2(2S_{1o}S_2+2S_{1e}S_{1o})\cdot(\sin 2\pi x-0.5\sin 4\pi x)\Big] \end{aligned} \quad \text{(A2.5)}$$

Although 3-symbol decision windows are used to improve the passband response, (A2.5) may be verified by inserting the Fourier transforms of Table A2.1 to obtain Feher's QPSK-1 PSD.

Time-domain	Pulse shape	Even + Odd	Fourier Transform, S(x), x=fT$_s$
$s_0(t-nT_s)$	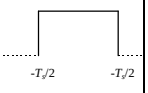	Function is even	$S_0(x)=\frac{T_s\sin\pi x}{\pi x}$
$s_1(t-nT_s)=$ $s_{1e}(t-nT_s)+$ $s_{1o}(t-nT_s)$	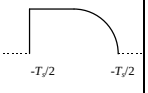	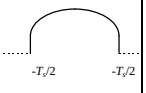 + 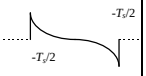	$S_{1e}(x)=0.5\left[S_0(x)+S_2(x)\right]$ $S_{1o}(x)=\frac{jT_s}{2\pi}\cdot$ $\left[\frac{1-\cos\pi x}{x}+\frac{2(2x-\sin\pi x)}{1-4x^2}\right]$
$s_2(t-nT_s)$	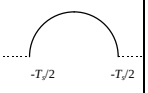	Function is even	$S_2(x)=\frac{2T_s\cos\pi x}{\pi(1-4x^2)}$

Table A2.1 Fourier transforms of 3-bit window pulse shapes for Feher's QPSK-1

REFERENCES

1. "Performance characteristics for intermediate data rate digital carriers using convolutional encoding/ Viterbi decoding and QPSK modulation (QPSK/IDR)," *Intelsat Earth Station Standards* (IESS), Document IESS-308 (Rev. 9), November 30, 1998.
2. K. Feher, *Wireless Digital Communications*, Prentice Hall, 1995, pp. 117-133.
3. F. Mintzer, "On half-band, third-band and *N*th band FIR filters and their design," *IEEE Trans. Accoust., Speech, Signal Processing*, vol. ASSP-30, pp. 734-738, Oct. 1982.
4. P.P. Vaidyanathan and T.Q. Nguyen, "Eigenfilters: A new approach to least-squares FIR filter design and applications including Nyquist filters," *IEEE trans. Circuits Syst.*, vol. CAS-34, no. 1, pp. 11-23, Jan. 1987.
5. S. Jayasimha and P.V.R. Narasimha Rao, "An iteration scheme for the design of equiripple *M*th-band FIR filters," *IEEE Trans. Sig. Proc.*, vol. SP-43, No. 8, August 1995.
6. K. Feher, *Telecommunications Measurements, Analysis and Instrumentation*, Prentice Hall, 1987, pp. 22-23.
7. "Performance characteristics for intermediate data rate digital carriers using rate 2/3 TCM/ 8PSK and Reed-Solomon outer coding (TCM/IDR)," *Intelsat Earth Station Standards* (IESS), Document IESS-310 (Rev. 1), November 30, 1998.
8. J. Holmes, *Coherent Spread Spectrum Systems*, Chapter 2, Reprint edition (May 1990) Krieger Publishing Company; ISBN: 0894644688.
9. S. Jayasimha and C.G. Hiremath, "Pseudo-QMF banks with near-equiripple performance," *IEEE Trans. on Signal Processing*, pp. 209-214, vol. 46. No. 1, January 1998.
10. S. Jayasimha, "Projection on convex sets approach to design of near-equiripple NPR banks," *Journal of the Indian Institute of Science*, vol. 79, No. 2, pp. 125-132, March-April 1999.